Research Article | Vol. 26, No. 6 | 19 Mar 2018 | OPTICS EXPRESS 7516
Optics EXPRESS

Highly efficient, cascaded extraction optical parametric amplifier

HUABAO CAO,[1,3] SZABOLCS TÓTH,[1,3,*] MIKHAIL KALASHNIKOV,[2] VLADIMIR CHVYKOV,[1] AND KÁROLY OSVAY[1]

[1]*ELI-ALPS, ELI-HU Nonprofit Ltd., Dugonics tér 13., H-6720 Szeged, Hungary*
[2]*Max-Born-Institut for Nonlinear Optics and Short Pulse Spectroscopy, Max-Born-Starsse 2a, 12489 Berlin, Germany*
[3]*These authors contributed equally to the paper*
[*]*szabolcs.toth@eli-alps.hu*

Abstract: The scheme of cascaded extraction optical parametric amplifier (CE-OPA) has been proposed as a final amplifier for high peak power laser systems. 4D numerical simulations show that conversion efficiency of a CE-OPA system pumped with a temporal Gaussian pump pulse is as close to the theoretical limit of quantum efficiency as a conventional OPA pumped with temporal flat-top pump pulse. The CE-OPA system is also similar to the conventional scheme in output energy stability and alignment sensitivity of the phase-matching angles, too. However, with the use of the CE-OPA scheme, the requirement of pump pulse shaping can be relaxed, leading to an overall higher plug in efficiency as well as compact design.

OCIS codes: (140.4480) Optical amplifiers; (190.4970) Parametric oscillators and amplifiers; (320.7110) Ultrafast nonlinear optics.

References and links

1. G. Ma, W. Dallari, A. Borot, F. Krausz, W. Yu, G. D. Tsakiris, and L. Veisz, "Intense isolated attosecond pulse generation from relativistic laser plasmas using few-cycle laser pulses," Phys. Plasmas **22**(3), 033105 (2015).
2. P. B. Corkum and F. Krausz, "Attosecond science," Nat. Phys. **3**(6), 381–387 (2007).
3. S. Kühn, M. Dumergue, S. Kahaly, S. Mondal, M. Füle, T. Csizmadia, B. Farkas, B. Major, Z. Várallyay, E. Cormier, M. Kalashnikov, F. Calegari, M. Devetta, F. Frassetto, E. Masson, L. Poletto, S. Stagira, C. Vozzi, M. Nisoli, P. Rudawski, S. Maclot, F. Campi, H. Wikmark, C. L. Arnold, C. M. Heyl, P. Johnsson, A. L'Huillier, R. Lopez-Martens, S. Haessler, M. Bocoum, F. Boehle, A. Vernier, G. Iaquaniello, E. Skantzakis, N. Papadakis, C. Kalpouzos, P. Tzallas, F. Lépine, D. Charalambidis, K. Varjú, K. Osvay, and G. Sansone, "The ELI-ALPS facility: the next generation of attosecond sources," J. Phys. At. Mol. Opt. Phys. **50**, 132002 (2017).
4. L. D. Lucchio, A. A. Andreev, and P. Gibbon, "Ion acceleration by intense, few-cycle laser pulses with nanodroplets," Phys. Plasmas **22**(5), 053114 (2015).
5. G. A. Mourou, T. Tajima, and S. V. Bulanov, "Optics in relativistic regime," Rev. Mod. Phys. **78**(2), 309–371 (2006).
6. S. K. Barber, J. van Tilborg, C. B. Schroeder, R. Lehe, H.-E. Tsai, K. K. Swanson, S. Steinke, K. Nakamura, C. G. R. Geddes, C. Benedetti, E. Esarey, and W. P. Leemans, "Measured Emittance Dependence on the Injection Method in Laser Plasma Accelerators," Phys. Rev. Lett. **119**(10), 104801 (2017).
7. P. A. Walker, P. D. Alesini, A. S. Alexandrova, M. P. Anania, N. E. Andreev, I. Andriyash, A. Aschikhin, R. W. Assmann, T. Audet, A. Bacci, I. F. Barna, A. Beaton, A. Beck, A. Beluze, A. Bernhard, S. Bielawski, F. G. Bisesto, J. Boedewadt, F. Brandi, O. Bringer, R. Brinkmann, E. Bründermann, M. Büscher, M. Bussmann, G. C. Bussolino, A. Chance, J. C. Chanteloup, M. Chen, E. Chiadroni, A. Cianchi, J. Clarke, J. Cole, M. E. Couprie, M. Croia, B. Cros, J. Dale, G. Dattoli, N. Delerue, O. Delferriere, P. Delinikolas, J. Dias, U. Dorda, K. Ertel, A. Ferran Pousa, M. Ferrario, F. Filippi, J. Fils, R. Fiorito, R. A. Fonseca, M. Galimberti, A. Gallo, D. Garzella, P. Gastinel, D. Giove, A. Giribono, L. A. Gizzi, F. J. Grüner, A. F. Habib, L. C. Haefner, T. Heinemann, B. Hidding, B. J. Holzer, S. M. Hooker, T. Hosokai, A. Irman, D. A. Jaroszynski, S. Jaster-Merz, C. Joshi, M. C. Kaluza, M. Kando, O. S. Karger, S. Karsch, E. Khazanov, D. Khikhlukha, A. Knetsch, D. Kocon, P. Koester, O. Kononenko, G. Korn, I. Kostyukov, L. Labate, C. Lechner, W. P. Leemans, A. Lehrach, F. Y. Li, X. Li, V. Libov, A. Lifschitz, V. Litvinenko, W. Lu, A. R. Maier, V. Malka, G. G. Manahan, S. P. D. Mangles, B. Marchetti, A. Marocchino, A. Martinez de la Ossa, J. L. Martins, F. Massimo, F. Mathieu, G. Maynard, T. J. Mehrling, A. Y. Molodozhentsev, A. Mosnier, A. Mostacci, A. S. Mueller, Z. Najmudin, P A P. Nghiem, F. Nguyen, P. Niknejadi, J. Osterhoff, D. Papadopoulos, B. Patrizi, R. Pattathil, V. Petrillo, M. A. Pocsai, K. Poder, R. Pompili, L. Pribyl, D. Pugacheva, S. Romeo, A. R. Rossi, E. Roussel, A. A. Sahai, P. Scherkl, U. Schramm, C. B. Schroeder, J. Schwindling, J. Scifo, L. Serafini, Z. M. Sheng, L. O. Silva, T. Silva, C. Simon, U. Sinha, A.

#309026 https://doi.org/10.1364/OE.26.007516
Journal © 2018 Received 13 Oct 2017; revised 2 Dec 2017; accepted 6 Dec 2017; published 15 Mar 2018

Optics EXPRESS

Specka, M. J. V. Streeter, E. N. Svystun, D. Symes, C. Szwaj, G. Tauscher, A. G. R. Thomas, N. Thompson, G. Toci, P. Tomassini, C. Vaccarezza, M. Vannini, J. M. Vieira, F. Villa, C.-G. Wahlström, R. Walczak, M. K. Weikum, C. P. Welsch, C. Wiemann, J. Wolfenden, G. Xia, M. Yabashi, L. Yu, J. Zhu, and A. Zigler, "Horizon 2020 EuPRAXIA design study," J. Phys. Conf. Ser. **874**, 012029 (2017).

8. X. Wang, R. Zgadzai, N. Fazel, S. A. Yi, X. Zhang, W. Henderson, Y.-Y. Chang, R. Korzekwa, H.-E. Tsai, C.-H. Pai, Z. Li, H. Quevedo, G. Dyer, E. Gaul, M. Martinez, A. Bernstein, T. Borger, M. Spinks, M. Donovan, S. Y. Kalmykov, V. Khudik, G. Shvets, T. Ditmire, and M. C. Downer, "Petawatt-laser-driven wakefield acceleration of electrons to 2 GeV in 10^{17} cm^{-3} plasma," AIP Conf. Proc. **1507**(1), 341–344 (2012).
9. B. M. Hegelich, G. Mourou, and J. Rafelski, "Probing the quantum vacuum with ultra intense laser pulses," Eur. Phys. J. Spec. Top. **223**(6), 1093–1104 (2014).
10. F. G. Patterson, J. Bonlie, D. Price, and B. White, "Suppression of parasitic lasing in large-aperture Ti:sapphire laser amplifiers," Opt. Lett. **24**(14), 963–965 (1999).
11. V. V. Lozhkarev, G. I. Freidman, V. N. Ginzburg, E. V. Katin, E. A. Khazanov, A. V. Kirsanov, G. A. Luchinin, A. N. Mal'shakov, M. A. Martyanov, O. V. Palashov, A. K. Poteomkin, A. M. Sergeev, A. A. Shaykin, and I. V. Yakovlev, "Compact 0.56 Petawatt laser system based on oiptocal parametric chirped puse amplification in KD*P crystals," Laser Phys. Lett. **4**(6), 421–427 (2007).
12. O. V. Chekhlov, J. L. Collier, I. N. Ross, P. K. Bates, M. Notley, C. Hernandez-Gomez, W. Shaikh, C. N. Danson, D. Neely, P. Matousek, S. Hancock, and L. Cardoso, "35 J broadband femtosecond optical parametric chirped pulse amplification system," Opt. Lett. **31**(24), 3665–3667 (2006).
13. L. Xu, L. Yu, X. Liang, Y. Chu, Z. Hu, L. Ma, Y. Xu, C. Wang, X. Lu, H. Lu, Y. Yue, Y. Zhao, F. Fan, H. Tu, Y. Leng, R. Li, and Z. Xu, "High-energy noncollinear optical parametric-chirped pulse amplification in LBO at 800 nm," Opt. Lett. **38**(22), 4837–4840 (2013).
14. X. Zeng, K. Zhou, Y. Zuo, Q. Zhu, J. Su, X. Wang, X. Wang, X. Huang, X. Jiang, D. Jiang, Y. Guo, N. Xie, S. Zhou, Z. Wu, J. Mu, H. Peng, and F. Jing, "Multi-petawatt laser facility fully based on optical parametric chirped-pulse amplification," Opt. Lett. **42**(10), 2014–2017 (2017).
15. C. Danson, D. Hillier, N. Hopps, and D. Neely, "Petawatt class lasers worldwide," High Power Laser Sci. Eng. **3**, e3 (2015).
16. B. Rus, P. Bakule, D. Kramer, J. Naylon, J. Thoma, J. T. Green, R. Antipenkov, M. Fibrich, J. Novák, F. Batysta, T. Mazanec, M. A. Drouin, K. Kasl, R. Baše, D. Peceli, L. Koubíková, P. Trojek, R. Boge, J. C. Lagron, Š. Vyhlídka, J. Weiss, J. Cupal, J. Hřebíček, P. Hříbek, M. Ďurák, J. Polan, M. Košelja, G. Korn, M. Horáček, J. Horáček, B. Himmel, T. Havlíček, A. Honsa, P. Korouš, M. Laub, C. Haefner, A. Bayramian, T. Spinka, C. Marshall, G. Johnson, S. Telford, J. Horner, B. Deri, T. Metzger, M. Schultze, P. Mason, K. Ertel, A. Lintern, J. Greenhalgh, C. Edwards, C. Hernandez-Gomez, J. Collier, T. Ditmire, E. Gaul, M. Martinez, C. Frederickson, D. Hammond, C. Malato, W. White, and J. Houžvička, "ELI-Beamlines: Development of next generation short-pulse laser systems," Proc. SPIE **9515**, 95150F (2015).
17. L. J. Waxer, V. Bagnoud, I. A. Begishev, M. J. Guardalben, J. Puth, and J. D. Zuegel, "High-conversion-efficiency optical parametric chirped-pulse amplification system using spatiotemporally shaped pump pulses," Opt. Lett. **28**(14), 1245–1247 (2003).
18. V. Bagnoud, I. A. Begishev, M. J. Guardalben, J. Puth, and J. D. Zuegel, "5 Hz, > 250 mJ optical parametric chirped-pulse amplifier at 1053 nm," Opt. Lett. **30**(14), 1843–1845 (2005).
19. J. Adamonis, R. Antipenkov, J. Kolenda, A. Michailovas, A. P. Piskarkas, and A. Varanavicius, "High-energy Nd:YAG-amplification system for OPCPA pumping," Quantum Electron. **42**(7), 567–574 (2012).
20. J. Adamonis, R. Antipenkov, J. Kolenda, A. Michailovas, A. P. Piskarkas, A. Varanavicius, and A. Zaukevičius, "Formation of flat-top picosecond pump pulses for OPCPA systems by cascade second harmonic generation," Lith. J. Phys. **52**(3), 193–202 (2012).
21. J. A. Fülöp, Zs. Major, B. Horváth, F. Tavella, A. Baltuška, and F. Krausz, "Shaping of picosecond pulses for pumping optical parametric amplification," Appl. Phys. B **87**(1), 79–84 (2007).
22. R. Budriūnas, T. Stanislauskas, J. Adamonis, A. Aleknavičius, G. Veitas, D. Gadonas, S. Balickas, A. Michailovas, and A. Varanavičius, "53 W average power CEP-stabilized OPCPA system delivering 5.5 TW few cycle pulses at 1 kHz repetition rate," Opt. Express **25**(5), 5797–5806 (2017).
23. P. Wnuk, Y. Stepanenko, and C. Radzewicz, "Multi-terawatt chirped pulse optical parametric amplifier with a time-shear power amplification stage," Opt. Express **17**(17), 15264–15273 (2009).
24. M. Schultze, T. Binhammer, G. Palmer, M. Emons, T. Lang, and U. Morgner, "Multi-μJ, CEP-stabilized, two-cycle pulses from an OPCPA system with up to 500 kHz repetition rate," Opt. Express **18**(26), 27291–27297 (2010).
25. H. Fattahi, C. Skrobol, M. Ueffing, Y. Deng, A. Schwarz, Y. Kida, V. Pervak, T. Metzger, Zs. Major, and F. Krausz, "High efficiency, multi-mJ, sub 10 fs, optical parametric amplifier at 3 kHz," in *Conference on Lasers and Electro-Optics*, OSA Technical Digest (online) (Optical Society of America, 2012), paper CTh1N.6.
26. H. Fattahi and R. Viskup, *High Energy and Short Pulse Lasers* (InTech, 2016), Chap. 3.
27. J. Ma, J. Wang, P. Yuan, G. Xie, K. Xiong, Y. Tu, X. Tu, E. Shi, Y. Zheng, and L. Qian, "Quasi-parametric amplification of chirped pulses based on a Sm^{3+}-doped yttrium calcium oxyborate crystal," Optica **2**(11), 1006–1009 (2015).
28. J. Ma, J. Wang, B. Zhou, P. Yuan, G. Xie, K. Xiong, Y. Zheng, H. Zhu, and L. Qian, "Broadband, efficient, and robust quasi-parametric chirped-pulse amplification," Opt. Express **25**(21), 25149–25164 (2017).

Optics EXPRESS

29. Y. Li, H. Zhong, J. Yang, S. Wang, and D. Fan, "Versatile backconversion-inhibited broadband optical parametric amplification based on an idler-separated QPM configuration," Opt. Lett. **42**(14), 2806–2809 (2017).
30. A. Andrianov, A. Szabo, A. Sergeev, A. Kim, V. Chvykov, and M. Kalashnikov, "Computationally efficient method for Fourier transform of highly chirped pulses for laser and parametric amplifier modeling," Opt. Express **24**(23), 25974–25982 (2016).
31. S. Banerjee, K. Ertel, P. D. Mason, P. J. Phillips, M. Siebold, M. Loeser, C. Hernandez-Gomez, and J. L. Collier, "High-efficiency 10 J diode pumped cryogenic gas cooled Yb:YAG multislab amplifier," Opt. Lett. **37**(12), 2175–2177 (2012).
32. S. Banerjee, P. D. Mason, K. Ertel, P. Jonathan Phillips, M. De Vido, O. Chekhlov, M. Divoky, J. Pilar, J. Smith, T. Butcher, A. Lintern, S. Tomlinson, W. Shaikh, C. Hooker, A. Lucianetti, C. Hernandez-Gomez, T. Mocek, C. Edwards, and J. L. Collier, "100 J-level nanosecond pulsed diode pumped solid state laser," Opt. Lett. **41**(9), 2089–2092 (2016).
33. L. Zhang, G. Yu, H. Zhou, L. Li, M. Xu, B. Liu, S. Ji, L. Zhu, F. Liu, and X. Sun, "Study on rapid growth of 98% deuterated potassium dihydrogen phosphate (DKDP) crystals," J. Cryst. Growth **401**, 190–194 (2014).
34. V. V. Lozhkarev, G. I. Freidman, V. N. Ginzburg, E. V. Katin, E. A. Khazanov, A. V. Kirsanov, G. A. Luchinin, A. N. Mal'shakov, M. A. Martyanov, O. V. Palashov, A. K. Poteomkin, A. M. Sergeev, A. A. Shaykin, I. V. Yakovlev, S. G. Garanin, S. A. Sukharev, N. N. Rukavishnikov, A. V. Charukhchev, R. R. Gerke, and V. E. Yashin, "200 TW 45 fs laser based on optical parametric chirped pulse amplification," Opt. Express **14**(1), 446–454 (2006).
35. C. Skrobol, I. Ahmad, S. Klingebiel, C. Wandt, S. A. Trushin, Z. Major, F. Krausz, and S. Karsch, "Broadband amplification by picosecond OPCPA in DKDP pumped at 515 nm," Opt. Express **20**(4), 4619–4629 (2012).
36. J. A. Armstrong, N. Bloembergen, J. Ducuing, and P. S. Pershan, "Interaction between Light Waves in a Nonlinear Dielectric," Phys. Rev. **127**(6), 1918–1939 (1962).
37. I. N. Ross, P. Matousek, G. H. C. New, and K. Osvay, "Analysis and optimization of optical parametric chirped pulse amplification," J. Opt. Soc. Am. B **19**(12), 2945–2956 (2002).
38. T. Lang, A. Harth, J. Matyschok, T. Binhammer, M. Schultze, and U. Morgner, "Impact of temporal, spatial and cascaded effects on the pulse formation in ultra-broadband parametric amplifiers," Opt. Express **21**(1), 949–959 (2013).
39. M. Guardalben, J. Keegan, L. Waxer, V. Bagnoud, I. Begishev, J. Puth, and J. Zuegel, "Design of a highly stable, high-conversion-efficiency, optical parametric chirped-pulse amplification system with good beam quality," Opt. Express **11**(20), 2511–2524 (2003).
40. F. Tavella, A. Marcinkevičius, and F. Krausz, "Investigation of the superfluorescence and signal amplification in an ultrabroadband multiterawatt optical parametric chirped pulse amplifier system," New J. Phys. **8**(10), 219 (2006).
41. P. Matousek, B. Rus, and I. N. Ross, "Design of a Multi-Petawatt Optical Parametric Chirped Pulse Amplifier for the Iodine Laser ASTERIX IV," IEEE J. Quantum Electron. **36**(2), 158–163 (2000).
42. V. Bagnoud and F. Wagner, "Ultrahigh temporal contrast performance of the PHELIX petawatt facility," High Power Laser Sci. Eng. **4**(e39), 1–8 (2016).
43. B. Dromey, S. Kar, M. Zepf, and P. Foster, "The plasma mirror—A subpicosecond optical switch for ultrahigh power lasers," Rev. Sci. Instrum. **75**(3), 645–649 (2004).

1. Introduction

Repetition rated high peak power ultrashort pulses are requested for various research fields in physics including high order harmonic generation and particle acceleration [1–7]. Peak power in the petawatt range will enable electron acceleration to multi-GeV levels and explore the physics of vacuums [8, 9]. Most of the operating petawatt lasers are based on Ti:sapphire amplifiers due to the rather large emission spectrum and loose requirements on the pump laser. Thermal loads within the Ti:sapphire crystal, despite the high thermal conductivity, set an upper bound for the achievable repetition rate, while parasitic lasing limits either the gain or the crystal diameter [10]. Chirped pulse OPA (OPCPA) systems have a much lower thermal load than Ti:sapphire laser amplifiers as quantum defects are dissipated as an idler beam. There is no transverse crystal size limit because parametric fluorescence is generated only inside the pump pulse time window and phase-mismatch prevents its subsequent amplification in the transverse direction. At the time of writing, there have been only a few petawatt class OPCPA systems operational [11–14] and a few more are planned [15, 16]. The small ratio of OPCPA based high peak power system relative to the Ti:S and neodymium based systems can be explained not only with the late arrival of the optical parametric technology but rather with the low efficiency of parametric amplification as well as the very specific pump laser requirements of high power OPCPA systems. The pump to signal

Optics EXPRESS

conversion efficiency is typically less than in Ti:sapphire amplifiers as the direction of the energy flow reverses before the full depletion of the pump pulse.

It has been demonstrated that conversion efficiency could be improved with shaping the pump pulse both in space and time [17, 18]. Pump pulse shaping [19–21] is readily use in current state-of-the-art OPCPA systems [22] but the shaping involves enlarged and complex pump laser chains and the efficiency, contrary to laser materials, still remains far from the theoretical limit of quantum efficiency. Time-shearing power amplification was demonstrated to achieve an extraction efficiency of 15% when OPCPA systems were pumped by few ns pulses (much longer than the seed) [23]. Recycling of the pump pulse from an OPA amplifier to the next amplifier crystal has improved also the conversion efficiency, especially of final amplifiers [24–26]. This technique, however, results in a considerably extended footprint of the overall OPCPA system as additional optics and delay stage is required. Deng and Krausz proposed a technique for simultaneous increase the amplified bandwidth and conversion efficiency. In this scheme the broadband seed is stretched to a few times of the pump pulse duration and different temporal/spectral parts of the stretched seed are amplified in subsequent crystals using the same pump pulse. Theoretical study of this solution predicts 57% efficiency (the quantum efficiency is 64% in their example) with 3 crystals. Experimental study of the same scheme with two crystal reached conversion efficiency of 33% [26]. Quasi parametric amplification (QPA) [27, 28], a recent new type of parametric amplification, works by doping the nonlinear crystal with ions which absorb the idler beam along the amplification process, supressing back conversion of the pump pulse. The experimental test has also revealed that QPA can be as efficient and insensitive to misalignment as Ti:sapphire amplifiers. This technology could be an effective solution for the petawatt or even exawatt peak power level OPCPA architectures at low repetition rate only, as the absorbed idler pulse will generate heat in the crystal. Another recently published work proposes an idler-separated quasi phase-matching scheme which consists from a sandwiched crystal chip and the idler wave straying away from the signal thus preventing back-conversion [29]. The numerical simulation of this solution predicts excellent amplified signal beam profiles and large gain bandwidth, however QPM crystals, such as PPLN or PPKTP are not available in large apertures, which prevents the use of this technique as a final amplifier in peak power laser systems.

In this paper a highly efficient and compact final amplifier design is proposed for high energy, high repetition rate laser amplifiers. In this cascaded extraction OPA (CE-OPA) the energy at the wings of pump beam is extracted in the first crystal (deep back-conversion at central region) while the signal beam regains energy from the central region of the pump in the second crystal. The scheme is very compact and high energy extraction efficiency can be achieved. The suitability and effectiveness of CE-OPA is shown by advanced 4D numerical simulations.

2. Modelling methods and parameters

A 4D numerical code for OPCPA was used that is based on split-step Fourier method. This uses a computationally efficient algorithm for Fourier transform of highly chirped pulses [30]. The code takes into account dispersion, diffraction, crystal anisotropy and parametric fluorescence as well, giving a very accurate description of three wave mixing. Conventional OPA and CE-OPA amplification have been simulated and compared using the same boundary parameters.

Table 1 lists the pulse parameters for two scenarios differing only with respect to the temporal shape of the pump pulse, that is, compare the ordinary Gaussian to an almost flat top one. The first case has an ordinary Gaussian temporal shape of 1^{st} order while in the second case a super Gaussian of 6^{th} order. The spatial shape in both cases was assumed to be a 6^{th} order Gaussian. The peak intensity of the pump pulse was kept at 1 GW/cm^2, to avoid optical damage, so that the pump energy has to be 1700 J and 1575 J in the first and second cases,

Optics EXPRESS

respectively. The pump wavelength and the central wavelength of the signal pulse was set to 515 nm and 910 nm, respectively. The former could be generated by e.g. frequency doubling of Yb:YAG laser pulses [31, 32]. DKDP was taken as the nonlinear medium as it is available in large aperture [33, 34]. Ultra-broadband amplification in a DKDP crystal has been demonstrated with type I. phase matching configuration [35] using a 96% deuterated DKDP crystal with a phase-matching and non-collinear angle of 37.44° and 1.06° respectively.

Table 1. Pulse Parameters used in modelling.

	Seed	Pump
Central wavelength (nm)	910	515
FWHM pulse duration (ns)	1 (Fourier-limit: 12fs)	1.2
FWHM bandwidth (nm)	100	narrow band
Gaussian order (time domain)	1	Case 1: 1 Case 2: 6
FWHM diameter (cm)	30	40
Gaussian order (space)	1	6
Peak intensity (GW/cm^2)	0.002	1
Energy (J)	2	Case 1: 1700 Case 2: 1575

3. Cascaded Extraction (CE-) OPA configuration

High power OPA technology has been the object of vast experimental and theoretical investigations [36–40], which reveal that an optimal crystal thickness in OPA systems are needed to reach the saturation regime of the amplifier and then the maximum conversion efficiency is also obtained. In most cases, the pump pulse does not deplete uniformly due to intensity variations in the pump temporal and spatial profiles. Figures 1(a)-1(d) show the evolution of a spatial 6th and temporal 1st order Gaussian pump pulse for the first case. For the highest conversion efficiency, a small portion of idler and signal photons are converted back into pump photons forming a central lobe in the pump's spatiotemporal structure (Fig. 1(c)). Consequently, a poorly depleted pump pulse wastes its useful energy content.

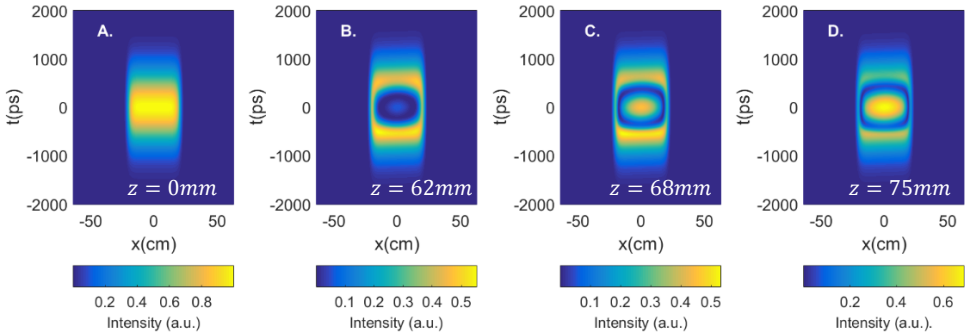

Fig. 1. The evolution of a spatial 6th and temporal 1st order Gaussian pump pulse during amplification at A. z = 0·L_{OPT}; B. z = 0.9· L_{OPT}; C. z = L_{OPT}; D. z = 1.1·L_{OPT}. L_{OPT} is the optimal crystal thickness, where the conversion efficiency is maximal. X is one dimension of the cross section of the pump beam.

Optics EXPRESS

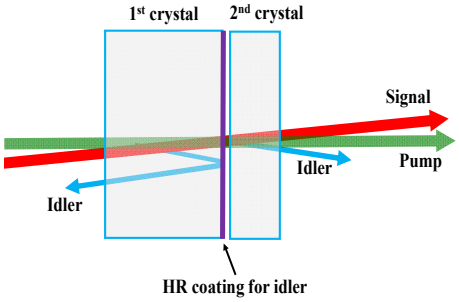

Fig. 2. Schematics of CE-OPA. The idler beam is reflected by the high reflection (HR) coating from the back side of the 1st crystal.

Figure 2 shows the proposed CE-OPA scheme which circumvents the poor pump depletion problem and increases the pump-to-signal conversion efficiency towards the theoretical quantum efficiency. CE-OPA utilizes two crystals with their thicknesses carefully chosen from numerical optimization. The first crystal is thicker than in a conventional OPA set-up and thus depleting the outer region of the pump pulse more effectively, allowing the central part to be almost fully back converted (Fig. 1(d)). Then the idler pulse has to be prevented from entering the second thinner crystal by a dichroic coating on the rear surface of the crystal or by being blocked after a certain distance while the idler and other beams have been well separated by the use of non-collinear phase-matching. The previously depleted outer pump region will remain empty as there is no idler to recombine with the signal thus the signal consumes the remaining energy from the central lobe of the pump pulse. Consequently, the extraction efficiency is high, leaving a highly depleted pump pulse behind.

It is worth mentioning that formally a similar scheme was used to avoid bandwidth narrowing in multistage OPCPA systems [41], where each stage was pumped separately by a dedicated pump line. The CE-OPA scheme is, however, optimized for efficient energy extraction from one pump pulse within one stage. CE-OPA also reduces gain narrowing and better energy and alignment stability is expected, which will be considered in detail in a later section.

4. Simulation results and discussion

4.1 Improvement of extraction efficiency

The optimal crystal thickness for conventional OPA can be easily determined by plotting the output signal energy versus the propagation distance (Fig. 3(a)). In CE-OPA optimal crystal thicknesses is obtained by varying the thickness of the 1st DKDP (Fig. 3(b)) from 70 mm up to 100 mm. For each crystal thickness, the envelope of the three dimensional pump, signal and idler field distributions are obtained from the numerical code and the output pump and signal fields served as the input fields for the 2nd DKDP. This way the optimal thickness of the second crystal (orange circles, Fig. 3) and the corresponding output energy of CE-OPA (blue crosses, Fig. 3) can be obtained as the function of the first crystal thickness. Optimization leads to the ideal CE-OPA crystal thicknesses of 86 mm and 32.5 mm for the first and second crystal respectively in the first temporal case and 80 mm and 28.5 mm in the second case respectively.

Optics EXPRESS

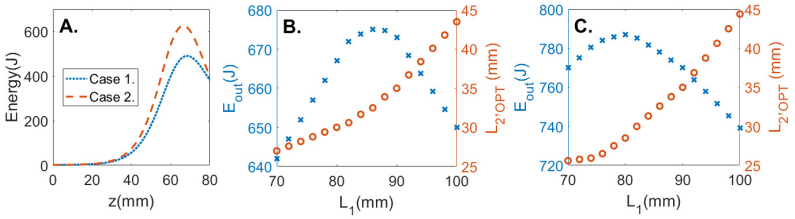

Fig. 3. A. Energy evolution of the signal pulse in OPA in both cases. Optimization process of CE-OPA in case 1(B) and case 2(C). The blue crosses correspond to the output energy and the orange circles correspond to the optimal second crystal thickness. L_1 – thickness of the 1st DKDP, $L_{2,\,OPT}$ – optimal thickness of the 2nd DKDP, E_{out} – output energy of CE-OPA

The optimal crystal thickness in a conventional OPA system is 68.5 mm and 66.5 mm for the first and second temporal cases respectively (Fig. 3(a)) and the output energies of 490 J and 627 J corresponds to 29% and 40% pump-to-signal conversion efficiencies respectively. The corresponding temporal shapes of the output signal (orange dotted line) and pump (blue continuous line) pulses are plotted in Figs. 4(a) and 4(d). For CE-OPA, the one dimensional cuts of the pump and signal intensities in time domain after the first crystal are plotted in Figs. 4(b) and 4(e) for the first and second case respectively and the exiting temporal profiles are shown in Figs. 4(c) and 4(f). The corresponding output energies are 675 J (case 1) and 787 J (case 2) and the pump-to-signal conversion efficiencies are 40% and 50%, respectively. These results show that the pump pulse is better used in CE-OPA and 2D sections of the output pump pulses have been made (Fig. 5) in order to show the difference in the pump depletion between conventional and CE-OPA. Figures 5(a) and 5(b), and Figs. 5(c) and 5(d) show the deviation between the two types of OPAs for case 1 and case 2, respectively. Figures 5(b) and 5(d) clearly show that for the CE-OPA method, there is a greater depletion in the region where the pump pulse overlaps with the signal pulse when compared to conventional OPA (Figs. 5(a) and 5(c)).

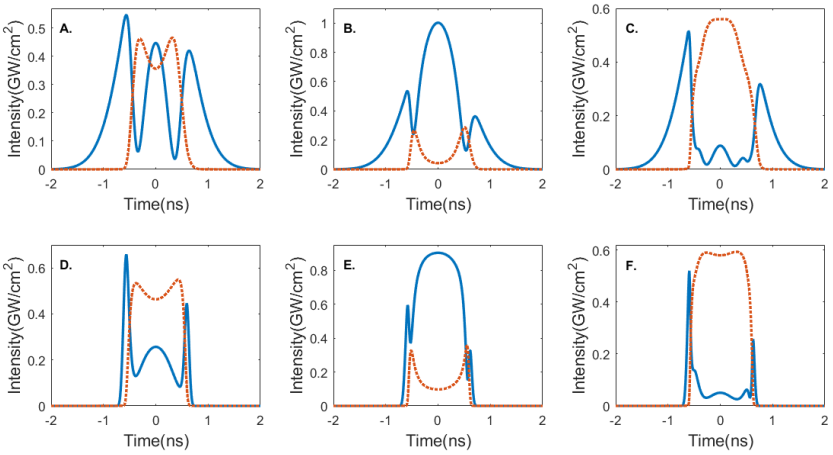

Fig. 4. Temporal shapes of output pulses in conventional OPA (A. and D) and CE-OPA after the 1st crystal (B and E) and after the 2nd crystal (C and F) for case 1 and case 2, respectively. The blue (orange) curve represents the temporal shape of the pump (signal) pulse.

Optics EXPRESS

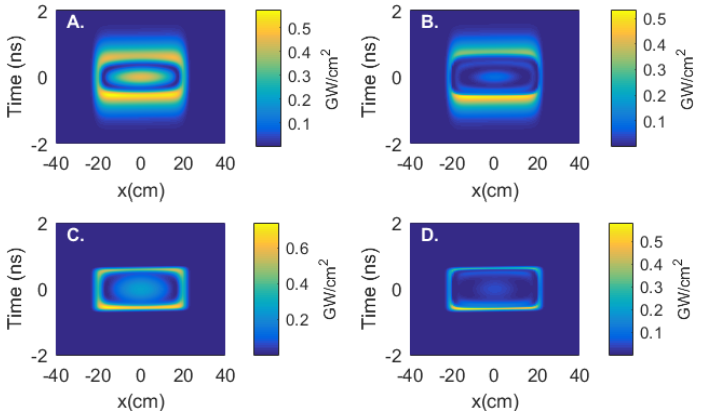

Fig. 5. The depletion of the pump pulse in conventional OPA (A, C) and in CE-OPA (B, D) with respect to case 1 and case 2.

Table 2. Results of the modelling.

Case (#)	OPA type	L1 (mm)	L2 (mm)	η (%)
1.	OPA	68.5		29
	CE-OPA	86	32.5	40
2.	OPA	66.5		40
	CE-OPA	80	28.5	50

Table 2 shows that the proposed amplifier scheme is 10% more efficient than conventional OPA. Furthermore, CE-OPA pumped with temporally 1st order pump pulse (1st case) reaches the same efficiency than a conventional OPA pumped with a temporally flat-top pump pulse (2nd case). Therefore, CE-OPA is a simple alternative method for temporal pump pulse shaping, thus could reduce the complexity of the pump system. Finally, the energy extraction from pump to signal almost reaches the quantum efficiency, 56.6% at these wavelengths, in the 2nd case using CE-OPA.

4.2 Spectral shape and temporal contrast

Figures 6(a) and 6(b) shows the spectra and residual phases of CE-OPA amplified pulses in the 1st and 2nd cases together with those of a conventional OPA. Under the standard condition when the duration of pump and chirped seed pulses are comparable, the amplified bandwidth for both schemes are slightly narrower than the input spectrum (dashed line). The Fourier-limited pulse duration calculated from the spectra on Fig. 6 after the conventional OPA is 20.2 fs and 20 fs in the 1st and 2nd case, respectively. The CE-OPA amplified spectra are slightly broader than that of OPA. Fourier-limited pulse durations in the 1st case (Fig. 6(a)) and 2nd case (Fig. 6(b)) are 18.8 fs and 19.8 fs, respectively. Therefore, tens of PW peak power pulses can be generated with compression efficiency of 50%. The residual spectral phase was calculated assuming a pulse compression up to 4th order dispersion compensation. One can establish that the residual spectral phase for CE-OPA pulses are less distorted at the wings compared to conventional OPA.

Optics EXPRESS

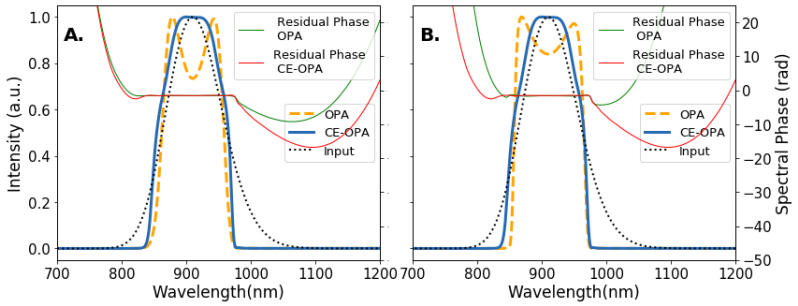

Fig. 6. Signal spectrums after amplification in OPA and CE-OPA and residual spectral phase after compression in the 1st (A) and 2nd (B) case, respectively.

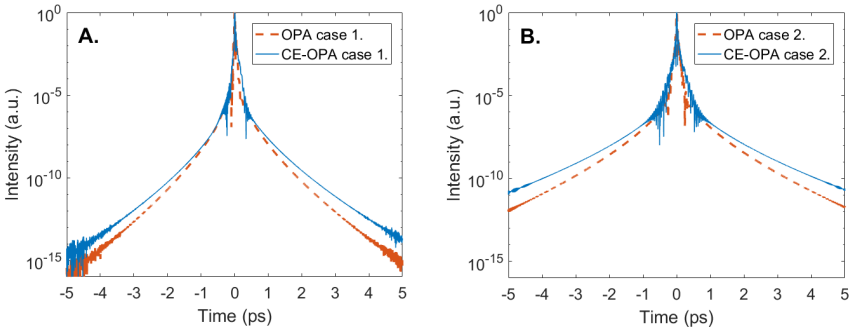

Fig. 7. Compressed pulse shapes on a logarithmic scale in the 1st (A) and 2nd (B) cases. The orange and blue curves represent the amplified signal in OPA and CE-OPA. The near-time signal contrast after CE-OPA is somewhat deteriorated as expected due to the more pronounced steepening of the fronts of the amplified spectrum.

Amplification in a saturated OPA with temporally supergaussian pump results in intense steepening of the spectral edges and the whole spectrum is close to rectangular shape. This effect deteriorates the close-to-peak temporal contrast of the compressed pulse and can also be observed in CE-OPA (Figs. 6(a) and 6(b), blue curves). The temporal profiles of CE-OPA and OPA are compared in Fig. 7. The amplification in CE-OPA (blue continuous curve) results in a slight degradation of temporal contrast of somewhat less than an order of magnitude. For case 1 (temporal Gaussian pump), the intensity at 5ps before the main peak is around 10^9W/cm^2 (contrast of 10^{-14}), which will not change the solid target condition before the arrival of the main pulse [42]. For case 2 (temporal supergaussian pump), the laser intensity (~10^{12}W/cm^2) at −5ps is still low enough to keep steep density gradient of many targets (e.g. gold, carbon [42]). If further steepening of the temporal front end is requested, one may in any case need to implement plasma mirrors [43].

4.3 Performance of CE-OPA for a real input pulse

In laboratory conditions the spectrum of a few cycle laser pulse is often far from the ideal Gaussian shape. In order to see how the spectral modulations influence the performance of CE-OPA, here we take the spectrum from a DKDP pre-amplifier seeded by a "Venteon Pulse One" Ti:Sa oscillator (black dotted curves in Fig. 8). Upon simulation, the procedure described in section 4.1 for finding the optimal crystal thicknesses was repeated here and the results are summarized in Table 3.

Optics EXPRESS

Table 3. Results of the modelling for a measured oscillator spectrum.

Case (#)	OPA type	L1 (mm)	L2 (mm)	η (%)
1.	OPA	66		19
	CE-OPA	77	27	28
2.	OPA	65		24
	CE-OPA	79	28	33

On the one hand, one can notice from the comparison of Tables 2 and 3, that in case of a real modulated spectrum the pump-to-signal conversion efficiencies are lower than in the case of a Gaussian. However, the efficiency of CE-OPA is still almost 10% higher than that of OPA for both cases. On the other hand, by applying one additional pre-amplification stage before the final amplifier it is possible to further smooth the spectrum and to achieve higher efficiency.

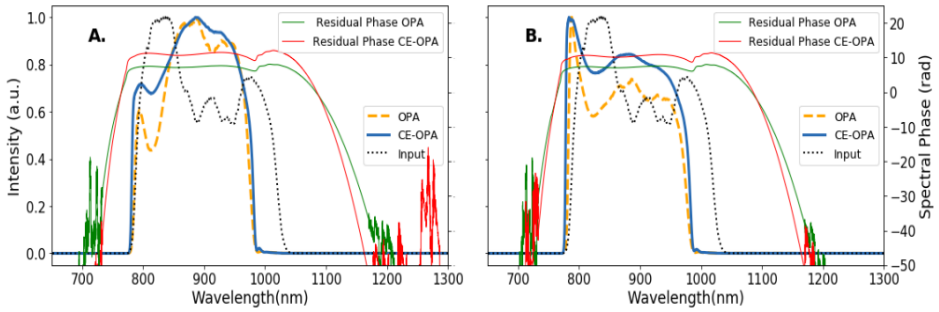

Fig. 8. Signal spectrums after amplification in OPA (orange dashed curve) and CE-OPA (blue curve) in the 1st (A) and 2nd (B) case respectively. The dotted curve represents the input signal spectrum. The green and red continuous curves are representing the residual phase of the amplified pulses after dispersion compensation up to 4th order.

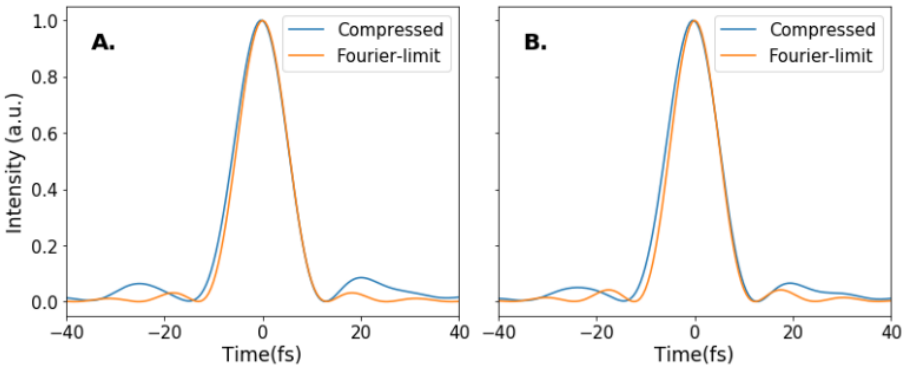

Fig. 9. Comparison of the compressed (blue) and Fourier-limited (orange) pulse shapes after amplification in CE-OPA in the 1st and 2nd cases respectively. The duration of the compressed and Fourier-limited pulses are 11.5 fs and 11 fs respectively.

The compressibility of the amplified pulses after CE-OPA with measured input signal spectrum was examined and presented in Figs. 8 and 9. For both cases (temporal Gaussian and supergaussian pump), CE-OPA achieved comparable bandwidth and flat residual spectral phase (dispersion was compensated still to 4th order). The compressed pulse durations were very close to the Fourier-limited ones, except small bumps at both sides of the main peak. Figure 10 shows the temporal contrast of the compressed pulse shapes of OPA (orange) and CE-OPA (blue), which are similar for both amplification schemes. The modulation of the measured input signal spectrum causes a rather flat pedestal, which can be obviously seen

Optics EXPRESS

from the contrast degradation of temporal contrast for case 1 (Fig. 10(a)) here compared to that of Gaussian spectrum signal (Fig. 7(a))

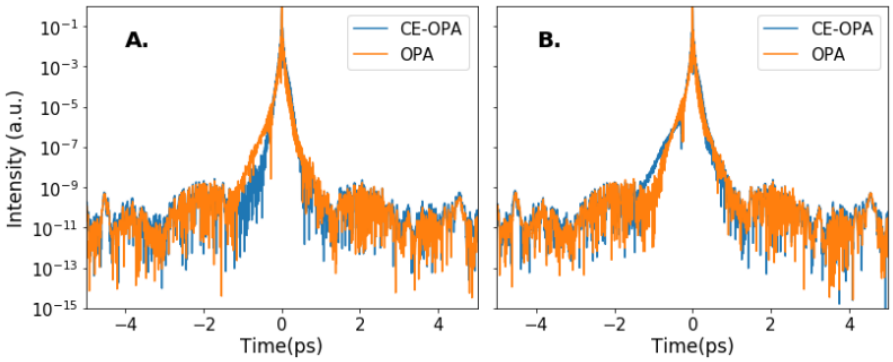

Fig. 10. Compressed pulse shapes on a logarithmic scale in the 1st (A) and 2nd (B) cases. The orange and blue curves represent the amplified signal in OPA and CE-OPA. In this realistic case there is no significant difference in the near-time contrast between the two amplifier types.

4.4 Output energy stability and alignment sensitivity

The output energy stability and alignment sensitivity of CE-OPA are simulated when the pump pulse is 6th order Gaussian in time. In Fig. 11(a), it is shown that the extraction efficiency curve of CE-OPA is flatter than that of OPA. This indicates that CE-OPA is more likely to provide stable output energy, even if the input signal is unstable. The dependence of the output signal energy on the pump intensity (Fig. 11(b)), on the other hand shows linear correlation. Consequently, in order to reach stable output energy in CE-OPA pump intensity stabilization is required.

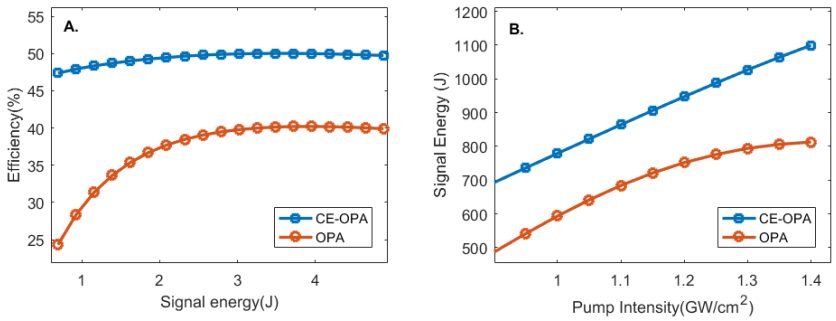

Fig. 11. Extraction efficiency versus input signal energy (A) and output signal energy versus pump intensity (B).

The alignment sensitivity of CE-OPA with respect to the detuning of the phase-matching (Θ) and non-collinear angle (α) was examined and compared to conventional OPA (Figs. 12(a) and 12(b)). Slight improvement in alignment sensitivity is observable which could be attributed to the fact that energy drop in the first crystal is partially compensated in the second one.

Optics EXPRESS

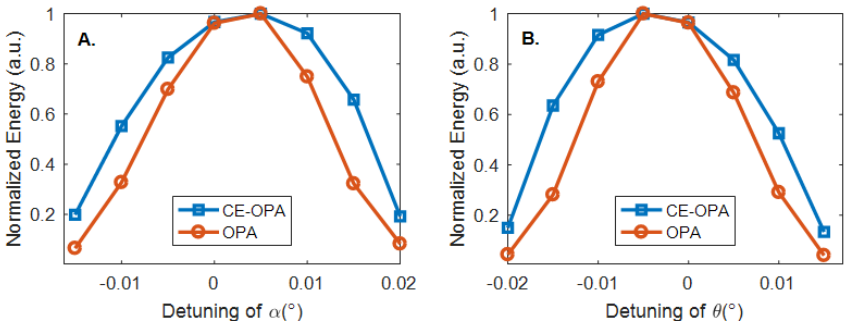

Fig. 12. Signal energy variation versus the detuning of non-collinear (A) and phase matching angle (B).

5. Conclusions

The CE-OPA configuration especially proposed for the last, power amplifier stages of PW class pulses, combines two nonlinear crystals in one stage. The first crystal allows enhanced depletion at the wings of the pump pulse. The idler pulse is blocked between the two crystals and thus the wave vector mismatch will be reset and starts from zero again in the 2nd crystal. This enables the signal pulse to consume the remaining energy from the central lobe of the pump and consequently, results in a greater depleted pump pulse. Numerical simulations suggest that approximately 10% higher efficiency could be achieved both for an ideal temporally Gaussian spectral shape as well as for a rather modulated measured pulse spectrum. Modelling was performed for DKDP crystals using a 4D numerical code. The input and output parameters of the calculations are summarized in Tables 1-3. CE-OPA was compared to a conventional OPA in two different temporal shapes. The first case is a first order Gaussian shape and the second is a sixth order Gaussian shape.

The highest efficiency, 50%, achieved in the second scheme is very close to the quantum efficiency (56.6%). Furthermore, CE-OPA pumped with a temporal Gaussian pulse is as effective as a conventional OPA pumped with a close to rectangular (temporal sixth order Gaussian) pump pulse. Consequently, the complexity of the pump system can be highly reduced with a CE-OPA setup instead of the conventional OPA system with carefully engineered pump shape. The output energy stability and alignment sensitivity of CE-OPA are comparable to the conventional OPA.

These results show that the CE-OPA configuration is a very promising amplifier design concept for the future multi-PW, few cycle laser systems.